Extracellular Microfibrils Control Osteoblast-supported Osteoclastogenesis by Restricting TGFβ Stimulation of RANKL Production*

Harikiran Nistala, Sui Lee-Arteaga, Silvia Smaldone, Gabriella Siciliano, and Francesco Ramirez[1]

From the Department of Pharmacology and Systems Therapeutics, Mount Sinai School of Medicine, New York, New York 10021

Mutations in fibrillin-1 or fibrillin-2, the major structural components of extracellular microfibrils, cause pleiotropic manifestations in Marfan syndrome and congenital contractural arachnodactyl, respectively. We recently found that fibrillin-1 and fibrillin-2 control bone formation by regulating osteoblast differentiation through the differential modulation of endogenous TGFβ and bone morphogenetic protein signals. Here, we describe *in vivo* and *ex vivo* experiments that implicate the fibrillins as negative regulators of bone resorption. Adult $Fbn2^{-/-}$ mice display a greater than normal osteolytic response to locally implanted lipopolysaccharide-coated titanium particles. Although isolated cultures of $Fbn2^{-/-}$ preosteoclasts exhibited normal differentiation and activity, these features were substantially augmented when mutant or wild-type preosteoclasts were co-cultured with $Fbn2^{-/-}$ but not wild-type osteoblasts. Greater osteoclastogenic potential of $Fbn2^{-/-}$ osteoblasts was largely accounted for by up-regulation of the *Rankl* gene secondary to heightened TGFβ activity. This conclusion was based on the findings that blockade of TGFβ signaling blunts *Rankl* up-regulation in $Fbn2^{-/-}$ osteoblasts and bones and that systemic TGFβ antagonism improves locally induced osteolysis in $Fbn2^{-/-}$ mice. Abnormally high *Rankl* expression secondary to elevated TGFβ activity was also noted in cultured osteoblasts from $Fbn1^{-/-}$ mice. Collectively our data demonstrated that extracellular microfibrils balance local catabolic and anabolic signals during bone remodeling in addition to implying distinct mechanisms of bone loss in Marfan syndrome and congenital contractural arachnodactyly.

Fibrillins are ubiquitous extracellular matrix (ECM)[2] glycoproteins that impart key physical properties to connective tissues and that control the local bioavailability of transforming growth factor-β (TGFβ) family members (1). The structural role of fibrillins is exerted through the temporal and hierarchical formation of tissue-specific assemblies (microfibrils and elastic fibers), whereas the instructive role reflects the ability of these extracellular molecules to bind TGFβ and bone morphogenetic protein (BMP) complexes (1). Fibrillin monomers self-assemble into microfibrils that associate or interact with several other matrix proteins, including fibulins, microfibril-associated glycoproteins (MAGPs), and latent TGFβ-binding proteins, as well as with elastin in the elastic fibers (2, 3). Binding of latent TGFβ-binding proteins to fibrillin and fibronectin assemblies indirectly targets latent TGFβ complexes to the ECM (4–6). Likewise, sequestration of BMPs in the matrix is mediated in part by direct interaction of their prodomains with the N-terminal regions of fibrillins (7).

Mutations of fibrillin genes in human patients and genetically engineered mice have been correlated with discrete phenotypic outcomes that reflect the dual roles of microfibrils in tissue formation, integrity, and remodeling (8). Like patients afflicted with Marfan syndrome (MFS; OMIM-154700), mice harboring mutations that affect the structure or synthesis of fibrillin-1 display dissecting aortic aneurysm, mitral valve prolapse, muscle hypoplasia, and developmental emphysema (9–11). These manifestations are in part accounted for by promiscuous Smad2/3 signaling secondary to improper ECM sequestration of latent TGFβ complexes (10, 12, 13). $Fbn2^{-/-}$ mice, on the other hand, recapitulate the small and large joint contractures that are the hallmark of individuals affected with congenital contractural arachnodactyly (CCA; OMIM-121050), a disease akin to but clinically distinct from MFS (14, 15). $Fbn2^{-/-}$ mice also display a skeletal patterning defect (syndactyly) that is absent in $Fbn1^{-/-}$ mice and that was genetically linked with decreased BMP7 signaling in the mesenchyme of early autopods (14, 16). Neither the relative patterns of fibrillin gene expression in various tissues, including the forming and mature skeleton, nor the established contributions of fibrillin proteins to microfibril biogenesis can fully account for the discrete phenotypic outcomes in MFS and CCA and their respective mouse models (2, 3). Hence, there is a need to explain how fibrillin-1 and fibrillin-2 contribute differently to the structural properties of extracellular microfibrils and their control of local TGFβ and BMP signals within various developmental and physiological contexts.

We recently began investigating the contribution of fibrillin-1 and fibrillin-2 to bone remodeling because of the following considerations. Microfibrils are abundantly deposited in the non-mineralized bone matrix (osteoid) laid down by differentiating preosteoblasts (17); low bone mass (osteopenia) is one of the few traits in common between MFS and CCA (15); and the

[1] To whom correspondence should be addressed. Tel.: 212-241-7237; Fax: 212-996-7214; E-mail: francesco.ramirez@mssm.edu.

[2] The abbreviations used are: ECM, extracellular matrix; ALK5, activin-like kinase-5 or TGFβ receptor I; BMM, bone marrow monocytes; BMP, bone morphogenetic protein; CCA, congenital contractural arachnodactyly; M-CSF, macrophage colony stimulating factor; MFS, Marfan syndrome; RANKL, receptor activator of nuclear factor-κ B ligand; TRAP, tartrate-resistant acid phosphatase; qPCR, quantitative PCR.
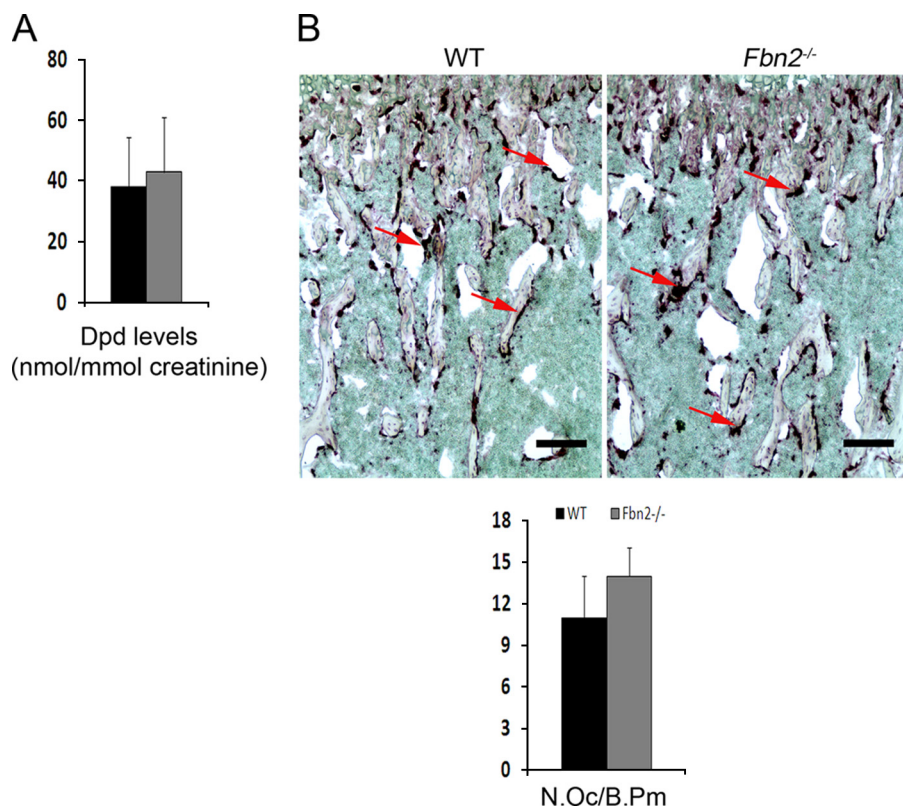
FIGURE 1. **Bone resorption in *Fbn2*$^{-/-}$ mice.** *A*, urinary concentration of deoxypyridinoline (*Dpd*) cross-links normalized to creatinine levels in wild-type (*black*) and mutant (*dark gray*) mice (*n* = 5 per each genotype). *B*, representative growth plate sections of TRAP-stained wild-type (WT) and *Fbn2*$^{-/-}$ tibias (*scale bar* = 200 μm) with *arrows* pointing to TRAP-positive cells; bar graphs below summarize the estimated number of osteoclasts per bone perimeter (*N.Oc/B.Pm*) in wild-type (*black*) and mutant (*gray*) bones (*n* = 5 per each genotype). *Error bars* represent ± S.D.

bone matrix is the preeminent storage site of TGFβ and BMP complexes (18). Bone remodeling is a complex and tightly regulated process that occurs throughout adult life in response to physiological stimuli and mechanical stresses and according to a locally coupled balance between bone resorption by osteoclasts and bone deposition by osteoblasts (19, 20). Extrinsic regulators of bone remodeling include circulating hormones, which promote bone anabolism and catabolism, signaling molecules, which are synthesized by bone cells or released locally from the ECM during bone resorption, and matrix components, which are directly or indirectly associated with osteoblast and osteoclast differentiation and with ECM mineralization and degradation (19, 20).

Relevant to the last group of extrinsic factors, gene function studies in mice have shown that collagen I fibrillogenesis is a critical contributor to bone mass and strength (21–26); that osteonectin supports osteoblast formation, maturation, and survival (27); that biglycan is involved in preosteoblast differentiation and osteoblast-supported osteoclastogenesis (28, 29); that osteopontin participates in stimulating osteoclast motility and bone resorption (30); and that MAGP1 restricts osteoclast differentiation and activity (31). Our own genetic studies have recently demonstrated that fibrillin-1 and fibrillin-2 support osteoblast maturation and bone formation by controlling local TGFβ and BMP bioavailability (32). On the one hand, *Fbn2*$^{-/-}$ mice were found to have one-third less bone mass and half the normal rate of bone formation because augmented TGFβ sig-

naling selectively interferes with osterix-driven collagen I production and osteoblast maturation. On the other hand, accelerated differentiation of *Fbn1*$^{-/-}$ osteoblasts in the presence of improper latent TGFβ activation was accounted for by slightly higher levels of osterix- and collagen I-coding transcripts and by a greater availability of otherwise matrix-bound BMPs.

The objective of the present study was to assess whether or not fibrillins may also be involved in regulating bone resorption. To this end, osteoclastogenesis was first evaluated in adult *Fbn2*$^{-/-}$ mice, and these findings were subsequently related to the behavior of mutant osteoclast precursors cultured alone or together with wild-type or mutant osteoblasts. Similar *in vitro* experiments were performed with bone cells isolated from *Fbn1*$^{-/-}$ mice. The results of these analyses demonstrated that microfibrils negatively regulate bone resorption by controlling osteoblast-supported osteoclastogenesis through a process that largely involves TGFβ-dependent stimulation of the osteoclastogenic factor receptor activator of nuclear factor-κ B ligand (RANKL). These findings, together with our parallel study of bone formation in fibrillin-deficient mice (32), significantly advance knowledge of the identity and relationship of local extrinsic factors that orchestrate bone formation, mineralization, and resorption during physiological remodeling and fracture healing.

EXPERIMENTAL PROCEDURES

Mice and Bone Resorption Measurements—The present studies employed *Fbn1*$^{-/-}$ and *Fbn2*$^{-/-}$ mice that were respectively bred into the C57/Bl6 and 129/SvEv genetic backgrounds (14, 16). Long bones from 3-month-old *Fbn2*$^{-/-}$ mice and wild-type littermates (*n* = 5 animals per each genotype) were processed and stained for tartrate-resistant acid phosphatase (TRAP) using the acid phosphatase staining kit (Sigma-Aldrich) according to the manufacturer's instructions. Numbers of surface osteoclasts (multinucleated TRAP-positive cells) in trabecular bone were evaluated with the aid of the OsteoMeasure analysis system (OsteoMetrics, Decatur, GA). Deoxypyridinoline cross-links were measured in morning urine of female mutant and control mice (*n* = 6 animals per each genotype) using the Pyrilinks-D immunoassay (Metra Biosystems, Mountain View, CA) and normalized to urinary creatinine content. Statistical analyses for these and all the other assays described below were performed using an unpaired *t* test (Microsoft Excel); significant association was defined when $p < 0.05$ compared with control.

Fibrillins Regulate Bone Resorption

In Vitro Osteoclastogenic Assays—For osteoclast differentiation assays ($n = 5$ assays per each genotype and each performed in duplicate), the bone marrow of 6–8-week-old wild-type or $Fbn2^{-/-}$ mice was flushed, and the monocyte fraction (bone marrow monocytes; BMM) was isolated by centrifugation, washed, seeded on 48-well plates at the concentration of 1.75×10^5 cells/well, and cultured for 7 days in differentiation medium, which includes minimum essential medium-α medium containing 15% FBS and 1% penicillin/streptomycin, 30 ng/ml macrophage colony-stimulating factor (M-CSF; R&D Systems, Minneapolis, MN), and 50 ng/ml recombinant RANKL (Sigma-Aldrich) (33). TRAP staining was performed using the acid phosphatase staining kit. For co-culture assays ($n = 3$ assays per each combination of genotypes and each performed in duplicate), calvarial osteoblasts were isolated from 4-day-old mutant or wild-type mice and plated on 24-well plates at a concentration of 5×10^4 cells/well. Once they reached confluence, BMM were plated at the concentration of 5×10^5 cells/well, and the co-cultures were further grown for 6–10 days in medium supplemented with 10^{-8} M 1,25-(OH)$_2$ vitamin D$_3$ and 10^{-6} M prostaglandin E2 (33). Multinucleated TRAP-positive cells were counted, and osteoclast activity was assessed by the pit formation assay using dentine slices (OsteoSite dentine slices, Immunodiagnostic Systems Inc., Fountain Hills, AR) that were preincubated in differentiation medium for 2 h (33). After 7 days of co-cultures, dentine slices were sonicated in 0.5 M ammonium hydroxide stained with toluidine blue for 2 min, washed with water, and photographed under a light microscope (Eclipse TE 200; Nikon, Yokahama, Japan). Resorbed areas were measured using NIH Image analysis software, normalized to the number of osteoclasts in the well, and expressed as the average resorbed area per cell.

In Vivo Osteolysis Assay—Implementation and analysis of experimentally induced osteolysis was carried out according to Bi *et al.* (29). Briefly, titanium particles with adherent lipopolysaccharide (LPS) endotoxin (8×10^6 particles/μl; Johnson Matthey, London, UK) or vehicle (25 μl of PBS) were implanted in the parietal bones of isoflurane-anesthetized 1-month-old wild-type or $Fbn2^{-/-}$ mice ($n = 3$ animals per each genotype), which were sacrificed 1 week later to harvest and process the calvarias for x-ray imaging and histology. In parallel experiments, mutant and wild-type mice ($n = 3$ animals per each genotype and treatment) were systemically treated with the TGFβ type I receptor (ALK5) inhibitor SD-208 (60 mg/kg; Tocris Biosciences, Ellisville, MO) or vehicle (1% methylcellulose, Sigma-Aldrich) twice daily for 7 days following LPS-induced osteolysis. The extent of osteolysis and the number of osteoclasts were evaluated by computer-aided histomorphometry of x-ray and light microscopy images using NIH Image J analysis software.

RNA Analyses—Real-time quantitative PCR (qPCR) employed total cellular RNA isolated using the RNeasy mini kit (Qiagen) and whose concentration and purity were determined spectrophotometrically (NanoDrop, Thermo Scientific, Waltham, MA). Reverse transcription assays for individual transcripts were each performed in triplicate on at least 3 independent RNA samples per genotype. Amplification assays were carried out with random hexamer primers (Invitrogen) and AffinityScript multiple temperature reverse transcriptase (Stratagene, La Jolla, CA) using 1 μg of total RNA according to manufacturer's instructions. The
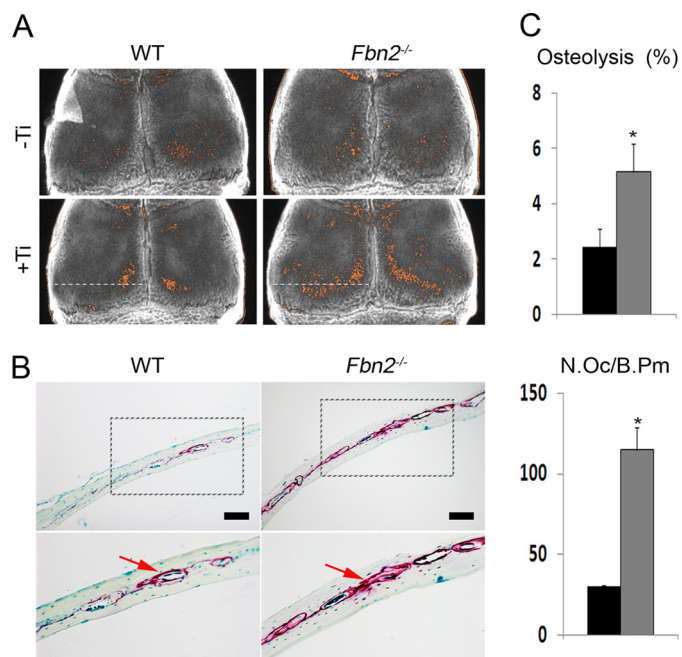

FIGURE 2. **Experimental osteolysis in $Fbn2^{-/-}$ mice.** *A*, illustrative x-ray radiographs of parietal bones from WT and $Fbn2^{-/-}$ mice that were sham-operated (*top; $-Ti$*) or implanted with LPS-titanium beads (*bottom; $+Ti$*) ($n = 3$ per each genotype and treatment). Resorption areas (*orange*) in each parietal bone were delineated in a blinded fashion from the x-ray radiographs using NIH Image-based histomorphometry. *B*, representative images of TRAP-stained parietal bones (*scale bar = 100 μm*) that were sectioned along the *white dotted line* shown in the x-ray images of *panel A*; below are magnified images (20$\times$) of the *boxed areas* above with *arrows* pointing to TRAP-positive cells. *C*, bar graphs summarize the percentage of osteolysis (resorbed bone over total bone area; *top*) and the number of osteoclasts per bone perimeter (*N.Oc/B.Pm, bottom*) in wild-type (*black*) and mutant (*dark gray*) mice. *Error bars* represent $\pm$ S.D., and *asterisks* signify statistically significant differences ($p < 0.05$).

cDNAs were amplified using SYBR Green Supermix with 6-carboxy-X-rhodamine (Fermentas, Glen Burnie, MD) on a Mastercycler ep realplex instrument (Eppendorf, Westbury, NY) using β-actin as an internal control. Amplification primers were purchased from SABiosciences, a Qiagen company (Frederick, MD) and included those specific for *Rankl* (PPM03047E), *Opg* (PPM03404E), *M-csf* (PPM02990E), and β-actin (PPM0245A). Thermal cycling conditions were incubation at 95 °C for 10 min followed by 40 cycles each consisting of 95 °C for 15 s (denaturation), 60 °C for 30 s (annealing), and 72 °C for 30 s (extension). In some experiments, qPCR assays were performed on total RNA purified from wild-type and $Fbn2^{-/-}$ osteoblasts ($n = 5$ independent samples per each genotype and treatment and each assayed in triplicate) plated and cultured for 4 days with 1 μM of the ALK5 inhibitor SB431542 (Sigma-Aldrich). For RNA interference (RNAi) experiments (34), wild-type and $Fbn2^{-/-}$ osteoblasts ($n = 3$ independent experiments per each genotype and treatment and each performed in duplicate) were transfected with 50 μM small interfering RNA (siRNA) specific for *Alk5* (10620312; Invitrogen) or non-targeting siRNA (J-040125; Dharmacon, Thermo Scientific). Likewise, wild-type calvarial osteoblasts ($n = 3$ independent experiments per each genotype and treatment and each performed in duplicate) were transfected with 50 μM siRNA specific for *Fbn1* or *Fbn2* (D-011034–03 and D-045311–03, respectively; Dharmacon, Thermo Scientific) along with the same non-targeting siRNA as control. Two days after siRNA transfection, total
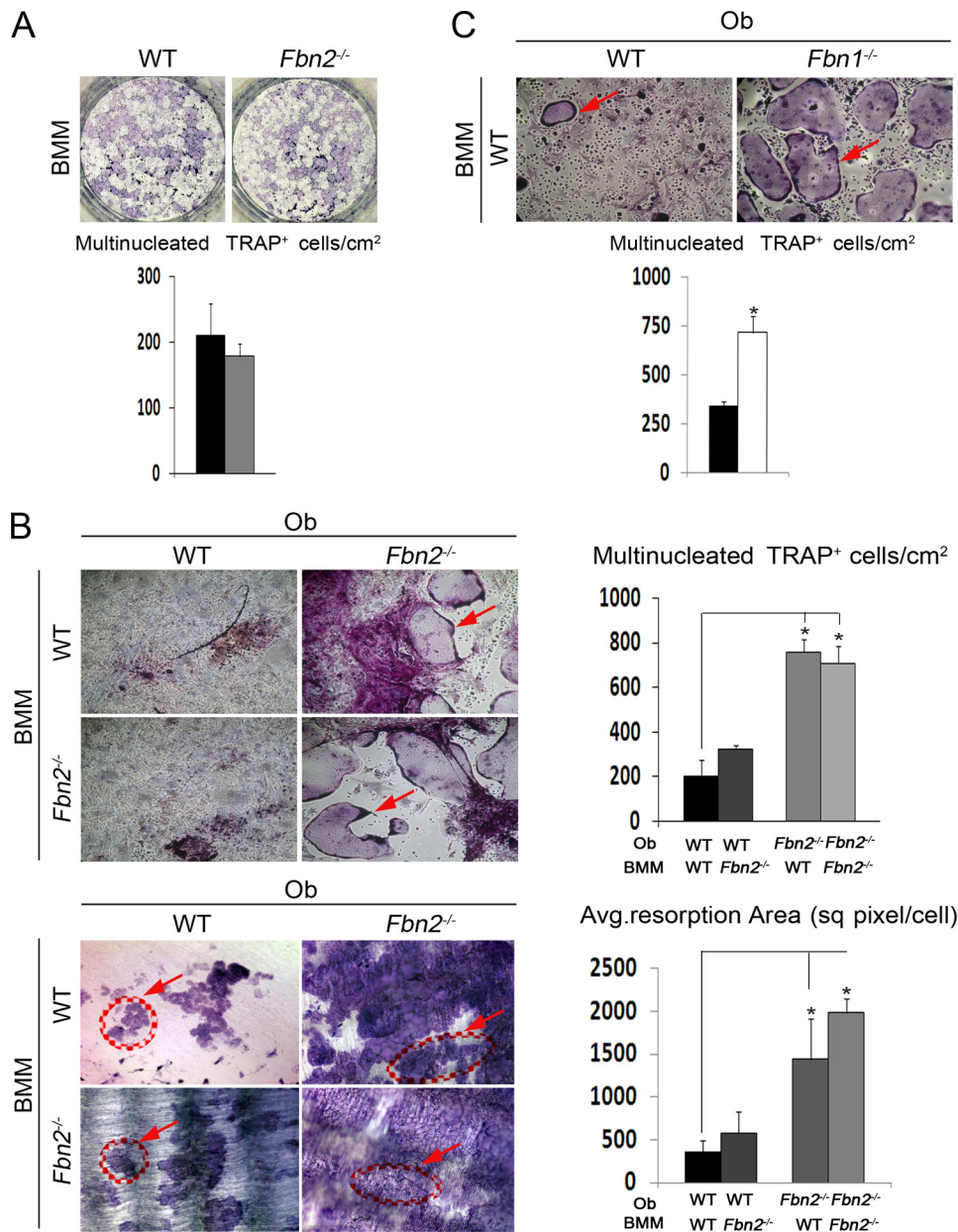
FIGURE 3. **Osteoclastogenesis in co-cultures with fibrillin-deficient osteoblasts.** *A*, osteoclast differentiation of BMM from WT and *Fbn2*$^{-/-}$ mice with bar graphs below summarizing the number of TRAP-positive multinucleated cells per cm^2 in control (*black*) and mutant (*gray*) samples (*n* = 5 per each genotype). *B*, osteoclast differentiation of WT or *Fbn2*$^{-/-}$ BMM co-cultured with WT or *Fbn2*$^{-/-}$ osteoblasts (*Ob*) showing TRAP-positive cells (*red arrow*; *top*) and toluidine blue-stained resorption pits (*red circles* with *arrows*; *bottom*); bar graphs on the *right* of the respective panels summarize the osteoclast number and the average resorbed area per cell (*n* = 3 per each genotype and experimental combination). *sq pixel*, square pixel. *C*, osteoclast differentiation of WT BMM co-cultured with WT or *Fbn1*$^{-/-}$ osteoblasts with *red arrow* pointing to TRAP-positive cells; bar graphs below summarize the number of TRAP-positive multinucleated cells per cm^2 in WT (*black*) and *Fbn1*$^{-/-}$ (*light gray*) samples (*n* = 3 per each genotype and experimental combination). *Error bars* represent ± S.D., and *asterisks* signify statistically significant differences (*p* < 0.05).

RNA was collected, and qPCR was employed to estimate the extent of gene silencing and the levels of *Rankl* transcripts. All qPCR data represent multiple biological replicates each analyzed in triplicate and expressed relative to the indicated controls arbitrarily averaged as 1 unit.

RESULTS

Fbn2$^{-/-}$ *Mice Display Increased Osteolytic Activity*— *Fbn2*$^{-/-}$ mice are viable and fertile, and by 3 months of age,

they display 27% less bone mass and a 55% reduction in bone formation rate, which cell culture experiments have correlated with severely impaired osteoblast maturation secondary to greater latent TGFβ activation (14, 32). Examination of two static parameters of bone resorption, urinary excretion of deoxypyridinoline cross-links and the number of TRAP-positive cells, failed to identify significant changes between 3-month-old *Fbn2*$^{-/-}$ mice and wild-type littermates (Fig. 1, *A* and *B*). An acute bone resorption response (osteolysis) was therefore elicited locally in *Fbn2*$^{-/-}$ mice to uncover potential changes in osteoclast activity (29). Specifically, LPS-coated titanium particles were implanted on the surface of parietal bones of 2-month-old *Fbn2*$^{-/-}$ and wild-type mice. A week later, the calvarias were harvested and examined by contact x-ray to visualize sites of LPS-induced osteolysis (Fig. 2*A*). Computer-aided quantitative resolution of the x-ray images revealed that osteolysis occurred more extensively in *Fbn2*$^{-/-}$ than wild-type calvarias (Fig. 2*B*). This conclusion was further corroborated by histological analyses of parietal bone sections that documented a statistically significant increase of TRAP-positive osteoclasts in mutant when compared with control samples (Fig. 2*C*). Taken at face value, these results suggested that heightened osteoclastogenesis is the major determinant of experimentally induced local osteolysis in *Fbn2*$^{-/-}$ mice.

Fibrillin Deficiency Stimulates Osteoblast-supported Osteoclastogenesis—To decipher the cellular mechanism underlying the above observations, osteoclast precursors (BMM) were first isolated from the bone marrow of 2-month-old *Fbn2*$^{-/-}$ mice and cultured *in vitro* either in the presence of M-CSF and RANKL, which stimulate osteoclast proliferation and differentiation, or together with mutant or wild-type calvarial osteoblasts, which synthesize both osteoclastogenic factors as well as the RANKL decoy osteoprotegerin (19, 20). Although no differences were noted in the number of TRAP-positive multinucleated cells between isolated wild-type and mutant BMM cultures, significantly more TRAP-positive multinucleated cells and larger resorp-

tion pits were observed when either wild-type or mutant BMM were co-cultured with mutant but not with wild-type osteoblasts (Fig. 3, *A* and *B*). The finding that BMM co-cultured with mutant osteoblasts are significantly more active than BMM in the presence of stimulatory factors implied that osteoblasts deficient for fibrillin-2 have greater than normal potential to support osteoclastogenesis. The results also suggested that this gain-of-function phenotype of $Fbn2^{-/-}$ osteoblasts is likely to translate in the elevated osteolytic response of $Fbn2^{-/-}$ mice.

Next, the above conclusion was evaluated in $Fbn1^{-/-}$ mice to establish whether or not both fibrillins play a negative role in controlling the osteoclastogenic potential of osteoblasts. In this case, however, the neonatal demise of $Fbn1^{-/-}$ mice limited our analysis to performing differentiation assays of wild-type BMM cultured together with mutant neonatal osteoblasts. Within this experimental limitation, the co-culture assays showed that osteoblasts deficient for fibrillin-1 stimulate osteoclastogenesis virtually to the same extent as those deficient for fibrillin-2 (Fig. 3C). Collectively these *in vitro* experiments suggested that a common molecular mechanism may be responsible for the enhanced osteoclastogenic potential of $Fbn1^{-/-}$ and $Fbn2^{-/-}$ osteoblasts.

Increased RANKL Expression Characterizes Fibrillin-deficient Osteoblasts—Local control of osteoclast activity by osteoblasts is exerted through the balanced synthesis of factors that promote (RANKL and M-CSF) or inhibit (osteoprotegerin) osteoclastogenesis (19, 20). Accordingly, we investigated whether changes in the relative expression of the *Rankl*, *Csf1*, and *Opg* genes could account for the ability of $Fbn1^{-/-}$ or $Fbn2^{-/-}$ calvarial osteoblasts to stimulate osteoclastogenesis more than the wild-type counterparts. In contrast to *Csf1* and *Opg*, we found that mutant osteoblasts produce significantly more *Rankl* mRNA than control cells (Fig. 4, *A* and *B*). We therefore concluded that loss of either fibrillin-1 or fibrillin-2 similarly stimulates RANKL production, and consequently, enhances the osteoclastogenic potential of mutant osteoblasts.

We have recently shown that primary calvarial osteoblasts produce and assemble both fibrillin-1 and fibrillin-2 microfibrils and that loss of either protein has virtually no effect on the expression levels of the other fibrillin gene (32). In contrast to the impaired maturation of $Fbn2^{-/-}$ osteoblasts, however, $Fbn1^{-/-}$ osteoblasts mature more rapidly than wild-type cells, and these opposite phenotypes can be replicated in wild-type osteoblasts in which either *Fbn1* or *Fbn2* expression is silenced by siRNA (32). Increased levels of *Rankl* mRNA in wild-type osteoblasts subject to *Fbn1* or *Fbn2* silencing further corroborated the phenotypic equivalence between siRNA-induced and germ line loss-of-function mutations of microfibrils, in addition to emphasizing the cell-autonomous nature of the *Rankl* up-regulation in fibrillin-deficient osteoblast cultures (Fig. 4C).

Heightened TGFβ Signaling Stimulates Experimental Osteolysis in $Fbn2^{-/-}$ Bones—Parallel work has equated the distinct maturation potential of $Fbn1^{-/-}$ and $Fbn2^{-/-}$ osteoblasts with heightened TGFβ and BMP signaling in the former cells and with greater TGFβ signaling in the latter cells (32). The finding that $Fbn1^{-/-}$ and $Fbn2^{-/-}$ osteoblasts share higher TGFβ
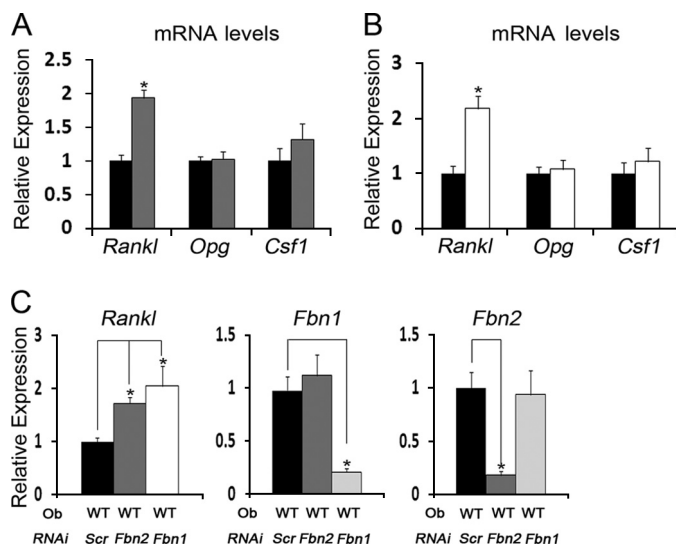

FIGURE 4. **RANKL expression in fibrillin-deficient osteoblasts.** *A* and *B*, steady-state levels of indicated transcripts in WT (*black*) and $Fbn2^{-/-}$ (*gray*) osteoblasts ($n = 6$ per each genotype; *A*) and in WT (*black*) and $Fbn1^{-/-}$ (*white*) osteoblasts ($n = 4$ per each genotype; *B*). Control WT values are arbitrarily averaged as 1 unit. *C*, steady-state levels of *Fbn* and *Rankl* transcripts in WT osteoblasts (*Ob*) transfected with non-targeting siRNA (*Scr*) or siRNA targeting *Fbn1* or *Fbn2* ($n = 3$ per each genotype and assay); control Scr values are arbitrarily averaged as 1 unit. *Error bars* represent ± S.D., and *asterisks* signify statistically significant differences ($p < 0.05$).
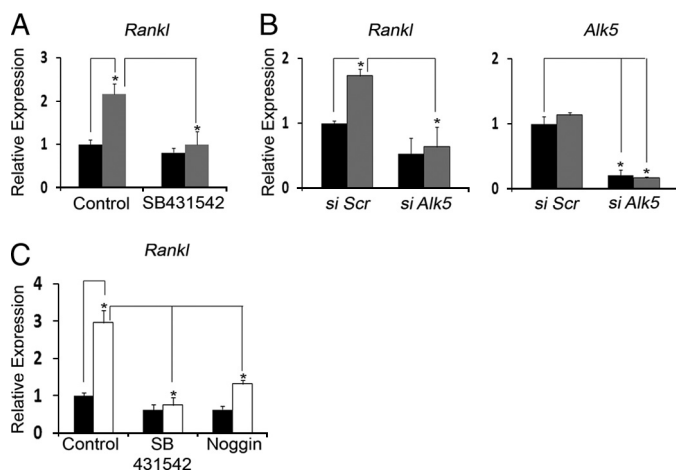

FIGURE 5. **TGFβ signaling regulates RANKL production.** *A* and *B*, steady-state levels of *Rankl* in WT (*black*) and $Fbn2^{-/-}$ (*gray*) osteoblasts cultured with or without the ALK5 kinase inhibitor SB431542 ($n = 5$ per each genotype; *A*) or transfected with non-targeting (*Scr*) or *Alk5*-targeting siRNA ($n = 5$ per each genotype; *B*). Histograms on the *right* of the latter panel indicate *Alk5* levels in osteoblasts transfected with non-targeting or *Alk5*-targeting siRNA. *C*, steady-state levels of *Rankl* in WT (*black*) and $Fbn1^{-/-}$ (*white*) osteoblast cultures treated with SB431542 (*SB*) or noggin ($n = 3$ per each genotype and treatment). WT values in control and non-targeting samples are each arbitrarily averaged as 1 unit. *Error bars* represent ± S.D., and *asterisks* signify statistically significant differences ($p < 0.05$).

activity and *Rankl* expression prompted us to investigate the possibility of a causal connection between these two cellular abnormalities. To this end, *Rankl* expression was first compared in $Fbn2^{-/-}$ and wild-type osteoblast cultures in which TGFβ signaling was inhibited by either chemical or genetic means. The results documented an appreciable normalization of *Rankl* expression in mutant osteoblasts that were either treated with the ALK5 kinase inhibitor SB431542 or transfected with *Alk5* siRNA (Fig. 5, *A* and *B*).
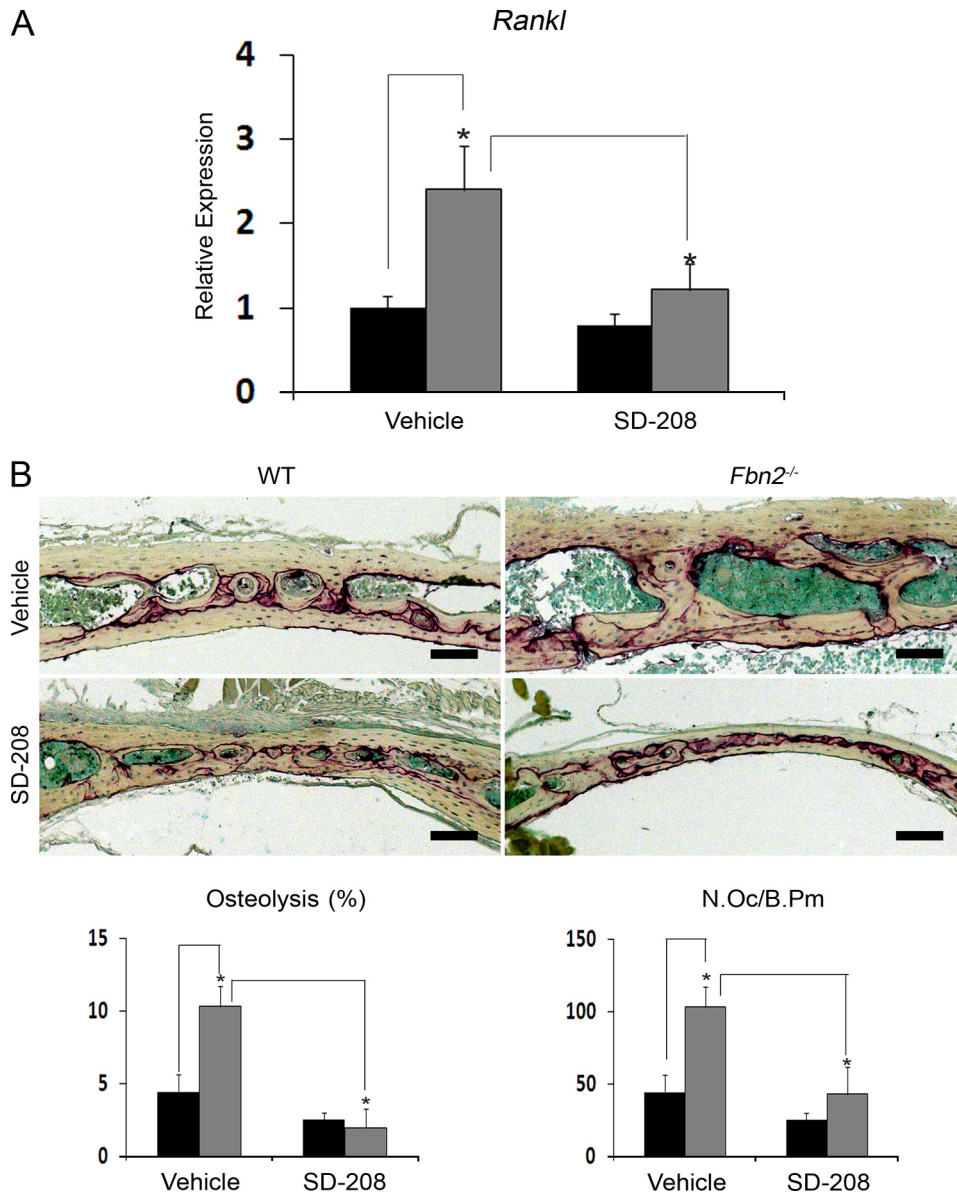
A

Rankl

B

FIGURE 6. **TGFβ signaling stimulates osteolysis in *Fbn2*$^{-/-}$ mice.** *A*, steady-state levels of *Rankl* transcripts in calvarial bones from adult wild-type (WT, *black*) and *Fbn2*$^{-/-}$ (*gray*) mice systemically treated for 2 months with either vehicle or the ALK5 kinase inhibitor SD-208 (*n* = 3 per each genotype and treatment). WT values in vehicle-treated samples are arbitrarily averaged as 1 unit. *B*, illustrative images of LPS-titanium-induced osteolysis in parietal bone sections of wild-type and *Fbn2*$^{-/-}$ mice systemically treated with vehicle or SD-208 (*scale bar* = 100 μm). Bar graphs below summarize the amount of absorbed tissue per bone surface and the number of osteoclasts per bone perimeter (*N.Oc/B.Pm*) in vehicle- and SD-208-treated wild-type (*black*) and mutant (*gray*) mice (*n* = 3 per each genotype and treatment). *Error bars* represent ± S.D., and *asterisks* signify statistically significant differences ($p < 0.05$).

Next, two independent lines of evidence correlated the *in vitro* data to the *in vivo* condition. First, qPCR analyses showed that systemic administration of the ALK5 kinase inhibitor SD-208 decreases considerably the abnormally high levels of *Rankl* transcripts noted in the bones of adult *Fbn2*$^{-/-}$ mice (Fig. 6A). Second, light microscopy documented that greater LPS-induced osteolysis was blunted in 2-month-old *Fbn2*-null mice that were systemically treated with SD-208 for 7 days following the implantation of titanium beads (Fig. 6B). Together the *ex vivo* and the *in vivo* experiments concurred in supporting the notion that loss of fibrillin-2 deposition in the forming osteoid augments the osteoclastogenic potential of mutant

osteoblasts by increasing *Rankl* expression, in part, through heightened TGFβ signaling.

The above conclusion was indirectly extended to mice deficient for fibrillin-1 by documenting that the ALK5 kinase inhibitor SB431542 normalizes the abnormal up-regulation of *Rankl* expression in *Fbn1*$^{-/-}$ osteoblasts (Fig. 5C). In line with published evidence from mice with disrupted BMP signaling (35, 36), *Rankl* expression was also downregulated in *Fbn1*$^{-/-}$ osteoblasts treated with the BMP antagonist noggin, but to a lesser extent than the TGFβ blockade (Fig. 5C). Taken at face value, this last finding suggested a probable cooperation between local TGFβ and BMP signals in regulating RANKL production by osteoblasts.

DISCUSSION

We have recently implicated fibrillin-1 and fibrillin-2 in the regulation of bone formation by respectively balancing the local release of TGFβ and BMP molecules and by restricting TGFβ bioavailability during osteogenic differentiation (32). This conclusion was based on the following findings. First, loss of fibrillin-2 impairs osteoblast maturation by increasing latent TGFβ activation, which in turn interferes with osterix-stimulated production of collagen I; second, loss of fibrillin-1 accelerates osteoblast differentiation by elevating TGFβ and BMP signaling to a degree that apparently restores the osterix-driven maturation process. Here, we showed that both fibrillins act as negative regulators of bone resorption and that both proteins exert most of their action through the modulation of TGFβ-dependent production of RANKL by osteoblasts. Together our studies therefore demonstrate that extracellular microfibrils are intimately involved in bone anabolism and catabolism by providing the structural scaffold that modulates local TGFβ and BMP bioavailability.

Extracellular regulation of TGFβ and BMP bioavailability is a critical but poorly characterized aspect of organ development and tissue remodeling (1). Current evidence indicates that latent TGFβ-binding proteins mediate targeting of latent TGFβ complexes to ECM components, including nascent fibronectin and fibrillin assemblies, whereas BMPs are directly

sequestered in the matrix through high affinity interactions between their prodomains and the N termini of fibrillins (4–7). Mutations that affect the structure or expression of fibrillins are therefore expected to dysregulate TGFβ and BMP signaling by interfering with the ECM-mediated processes of localizing and concentrating the ligands during organ development and releasing them in a timely fashion during tissue remodeling. This prediction is based on the characterization of fibrillin mutant mice, which has also documented the contextual specificity of microfibril regulation of TGFβ and BMP bioavailability (9–14, 33). Relevant to the latter point, mouse studies have implied that the phenotypic diversity of *Fbn1* and *Fbn2* mutant mice depends on yet to be defined mechanisms that specify which of all possible interactions between the growth factors and fibrillins may prevail in an individual tissue and at a given developmental stage or physiological process. Earlier examples of highly contextual interactions between extracellular microfibrils and growth factors include the unique promotion by fibrillin-2 of BMP signaling in the emerging autopods and the selective restriction by fibrillin-1 of TGFβ activity in the postnatal aortas, regenerating muscles, and developing lungs and mitral valves (10–14). The present investigations, together with our parallel study of bone formation in fibrillin-deficient mice (32), add another layer of complexity to the contextual specificity of microfibril control of TGFβ and BMP bioavailability by demonstrating that fibrillins have both unique and overlapping functions in modulating growth factor signaling during bone remodeling.

The influence of locally released TGFβ and BMP signals on the activity of and cross-talk between osteoblasts and osteoclasts remains largely undefined mostly because cell culture experiments have often yielded contradictory results, depending on the cell type and experimental conditions employed (18, 37). For example, osteoclasts co-cultured with osteoblasts have been reported to have opposite responses to high (inhibition) and low (stimulation) concentrations of TGFβ as a result of parallel changes in RANKL and osteoprotegerin production by osteoblasts (38–40). Our co-culture experiments adhere to a model in which differentiating preosteoclasts are continuously exposed to higher than normal amounts of RANKL and active TGFβ. Importantly, this *in vitro* evidence was corroborated *in vivo* by documenting the efficacy of systemic TGFβ antagonism to reduce both *Rankl* up-regulation and experimentally induced osteolysis in *Fbn2*$^{-/-}$ mice. Our results are also consistent with previous reports indicating that dysregulated TGFβ signaling in osteoblasts perturbs osteoclast activity and bone resorption in mice and that germ line ablation of a TGFβ-inducible transcription factor impairs RANKL production and osteoblast-supported osteoclastogenesis (41–43).

In addition to TGFβ, osteoclast precursors can also respond to BMP directly in isolated cultures or indirectly through BMP action on co-cultured osteoblasts (18). The latter mechanism was correlated with increased RANKL production *in vitro* and independently validated in mice in which BMP signaling is selectively inactivated in maturing osteoblasts (35, 44). Subsequent mouse studies suggested that BMP signaling in osteoblasts targets osteoclastogenesis directly by elevating *Rankl* expression and indirectly by stimulating sclerostin production

through inhibition of Wnt signaling (36). Our finding that noggin can partially inhibit *Rankl* transcription in *Fbn1*$^{-/-}$ osteoblasts is in agreement with these previous reports. Additionally, inhibition of *Rankl* up-regulation in *Fbn1*$^{-/-}$ osteoblasts by both SB431542 and noggin suggests that TGFβ and BMP signals cooperate in stimulating RANKL production, and this may conceivably translate into greater osteoclastogenic activity in *Fbn1*$^{-/-}$ than in *Fbn2*$^{-/-}$ mice. Although we are unable to evaluate osteolysis in *Fbn1*$^{-/-}$ mice, we can reasonably assume that the same abnormality may apply to *Fbn1* mutant mice that model adult MFS (9, 45). Along these same lines, one would expect that MFS or CCA patients may be at a greater risk than healthy individuals for implant wear-induced osteolysis and that TGFβ antagonism may be an effective means to manage this and related orthopedic problems. Indeed proof-of-concept experiments in mice have recently shown that systemic ALK5 inhibition has both anabolic and anti-catabolic effects on bone with the net effect of improving bone fracture resistance (46).

In summary, the present study identifies the fibrillin microfibrils as the first extrinsic factor that links together targeting of TGFβ and BMP complexes to the bone matrix with contextual specification of their respective signals and with osteoblast-promoted formation and degradation of the bone matrix (Fig. 6). This finding sheds new light on the extracellular mechanisms that coordinate the timely release and calibrate the threshold levels of TGFβ and BMP signals during bone remodeling. As such, this information has great potential to improve the design of therapeutic interventions to ameliorate bone loss and of bioengineered formulations to improve bone repair.

REFERENCES

1. Ramirez, F., and Rifkin, D. B. (2009) *Curr. Opin. Cell Biol.* **21,** 616–622
2. Hubmacher, D., Tiedemann, K., and Reinhardt, D. P. (2006) *Curr. Top. Dev. Biol.* **75,** 93–123
3. Ramirez, F., and Sakai, L. Y. (2010) *Cell Tissue Res.* **339,** 71–82
4. Taipale, J., Saharinen, J., Hedman, K., and Keski-Oja, J. (1996) *J. Histochem. Cytochem.* **44,** 875–889
5. Isogai, Z., Ono, R. N., Ushiro, S., Keene, D. R., Chen, Y., Mazzieri, R., Charbonneau, N. L., Reinhardt, D. P., Rifkin, D. B., and Sakai, L. Y. (2003) *J. Biol. Chem.* **278,** 2750–2757
6. Dallas, S. L., Sivakumar, P., Jones, C. J., Chen, Q., Peters, D. M., Mosher, D. F., Humphries, M. J., and Kielty, C. M. (2005) *J. Biol. Chem.* **280,** 18871–18880
7. Sengle, G., Charbonneau, N. L., Ono, R. N., Sasaki, T., Alvarez, J., Keene, D. R., Bächinger, H. P., and Sakai, L. Y. (2008) *J. Biol. Chem.* **283,** 13874–13888
8. Ramirez, F., and Dietz, H. C. (2007) *Curr. Opin. Genet. Dev.* **17,** 252–258
9. Pereira, L., Lee, S. Y., Gayraud, B., Andrikopoulos, K., Shapiro, S. D., Bunton, T., Biery, N. J., Dietz, H. C., Sakai, L. Y., and Ramirez, F. (1999) *Proc. Natl. Acad. Sci. U.S.A.* **96,** 3819–3823
10. Neptune, E. R., Frischmeyer, P. A., Arking, D. E., Myers, L., Bunton, T. E., Gayraud, B., Ramirez, F., Sakai, L. Y., and Dietz, H. C. (2003) *Nat. Genet.* **33,** 407–411
11. Ng, C. M., Cheng, A., Myers, L. A., Martinez-Murillo, F., Jie, C., Bedja, D.,

Gabrielson, K. L., Hausladen, J. M., Mecham, R. P., Judge, D. P., and Dietz, H. C. (2004) *J. Clin. Invest.* **114,** 1586–1592

12. Habashi, J. P., Judge, D. P., Holm, T. M., Cohn, R. D., Loeys, B. L., Cooper, T. K., Myers, L., Klein, E. C., Liu, G., Calvi, C., Podowski, M., Neptune, E. R., Halushka, M. K., Bedja, D., Gabrielson, K., Rifkin, D. B., Carta, L., Ramirez, F., Huso, D. L., and Dietz, H. C. (2006) *Science* **312,** 117–121

13. Cohn, R. D., van Erp, C., Habashi, J. P., Soleimani, A. A., Klein, E. C., Lisi, M. T., Gamradt, M., ap Rhys, C. M., Holm, T. M., Loeys, B. L., Ramirez, F., Judge, D. P., Ward, C. W., and Dietz, H. C. (2007) *Nat. Med.* **13,** 204–210

14. Arteaga-Solis, E., Gayraud, B., Lee, S. Y., Shum, L., Sakai, L., and Ramirez, F. (2001) *J. Cell Biol.* **154,** 275–281

15. Ramirez, F., and Arteaga-Solis, E. (2008) in *Primer on the Metabolic Bone Diseases and Disorders of Mineral Metabolism* (Rosen, C., ed) 7th Ed., pp. 450–454, ASBMR Publications, Washington, D. C.

16. Carta, L., Pereira, L., Arteaga-Solis, E., Lee-Arteaga, S. Y., Lenart, B., Starcher, B., Merkel, C. A., Sukoyan, M., Kerkis, A., Hazeki, N., Keene, D. R., Sakai, L. Y., and Ramirez, F. (2006) *J. Biol. Chem.* **281,** 8016–8023

17. Kitahama, S., Gibson, M. A., Hatzinikolas, G., Hay, S., Kuliwaba, J. L., Evdokiou, A., Atkins, G. J., and Findlay, D. M. (2000) *Bone* **27,** 61–67

18. Alliston, T., Piek, E., and Derynck, R. (2008). in *The TGFβ Family* (Derynck, R., and Miyazono, K., eds) pp. 667–723, Cold Spring Harbor Laboratory Press, Cold Spring Harbor, NY

19. Harada, S., and Rodan, G. A. (2003) *Nature* **423,** 349–355

20. Raggatt, L. J., and Partridge, N. C. (2010) *J. Biol. Chem.* **285,** 25103–25108

21. Bonadio, J., Saunders, T. L., Tsai, E., Goldstein, S. A., Morris-Wiman, J., Brinkley, L., Dolan, D. F., Altschuler, R. A., Hawkins, J. E., Jr., and Bateman, J. F. (1990) *Proc. Natl. Acad. Sci. U.S.A.* **87,** 7145–7149

22. Chipman, S. D., Sweet, H. O., McBride, D. J., Jr., Davisson, M. T., Marks, S. C., Jr., Shuldiner, A. R., Wenstrup, R. J., Rowe, D. W., and Shapiro, J. R. (1993) *Proc. Natl. Acad. Sci. U.S.A.* **90,** 1701–1705

23. Morello, R., Bertin, T. K., Chen, Y., Hicks, J., Tonachini, L., Monticone, M., Castagnola, P., Rauch, F., Glorieux, F. H., Vranka, J., Bächinger, H. P., Pace, J. M., Schwarze, U., Byers, P. H., Weis, M., Fernandes, R. J., Eyre, D. R., Yao, Z., Boyce, B. F., and Lee, B. (2006) *Cell* **127,** 291–304

24. Murakami, T., Saito, A., Hino, S., Kondo, S., Kanemoto, S., Chihara, K., Sekiya, H., Tsumagari, K., Ochiai, K., Yoshinaga, K., Saitoh, M., Nishimura, R., Yoneda, T., Kou, I., Furuichi, T., Ikegawa, S., Ikawa, M., Okabe, M., Wanaka, A., and Imaizumi, K. (2009) *Nat. Cell Biol.* **11,** 1205–1211

25. Choi, J. W., Sutor, S. L., Lindquist, L., Evans, G. L., Madden, B. J., Bergen, H. R., 3rd, Hefferan, T. E., Yaszemski, M. J., and Bram, R. J. (2009) *Plos Genet.* **5,** e1000750

26. Sohaskey, M. L., Jiang, Y., Zhao, J. J., Mohr, A., Roemer, F., and Harland, R. M. (2010) *J. Cell Biol.* **189,** 511–525

27. Delany, A. M., Kalajzic, I., Bradshaw, A. D., Sage, E. H., and Canalis, E. (2003) *Endocrinology* **144,** 2588–2596

28. Xu, T., Bianco, P., Fisher, L. W., Longenecker, G., Smith, E., Goldstein, S., Bonadio, J., Boskey, A., Heegaard, A. M., Sommer, B., Satomura, K., Dominguez, P., Zhao, C., Kulkarni, A. B., Robey, P. G., and Young, M. F. (1998) *Nat. Genet.* **20,** 78–82

29. Bi, Y., Nielsen, K. L., Kilts, T. M., Yoon, A., A Karsdal, M., Wimer, H. F., Greenfield, E. M., Heegaard, A. M., and Young, M. F. (2006) *Bone* **38,** 778–786

30. Chellaiah, M. A., Kizer, N., Biswas, R., Alvarez, U., Strauss-Schoenberger, J., Rifas, L., Rittling, S. R., Denhardt, D. T., and Hruska, K. A. (2003) *Mol. Biol. Cell* **14,** 173–189

31. Craft, C. S., Zou, W., Watkins, M., Grimston, S., Brodt, M. D., Broekelmann, T. J., Weinbaum, J. S., Teitelbaum, S. L., Pierce, R. A., Civitelli, R., Silva, M. J., and Mecham, R. P. (2010) *J. Biol. Chem.* **285,** 23858–23867

32. Nistala, H., Lee-Arteaga, S., Smaldone, S., Siciliano, G., Carta, L., Ono, R., Sengle, G., Arteaga-Solis, E., Levasseur, R., Ducy, P., Sakai, L. Y., Karsenty, G., and Ramirez, F. (2010) *J. Cell Biol.*, in press

33. Wang, X., Kua, H. Y., Hu, Y., Guo, K., Zeng, Q., Wu, Q., Ng, H. H., Karsenty, G., de Crombrugghe, B., Yeh, J., and Li, B. (2006) *J. Cell Biol.* **172,** 115–125

34. Carta, L., Smaldone, S., Zilberberg, L., Loch, D., Dietz, H. C., Rifkin, D. B., and Ramirez, F. (2009) *J. Biol. Chem.* **284,** 5630–5636

35. Mishina, Y., Starbuck, M. W., Gentile, M. A., Fukuda, T., Kasparcova, V., Seedor, J. G., Hanks, M. C., Amling, M., Pinero, G. J., Harada, S., and Behringer, R. R. (2004) *J. Biol. Chem.* **279,** 27560–27566

36. Kamiya, N., Ye, L., Kobayashi, T., Mochida, Y., Yamauchi, M., Kronenberg, H. M., Feng, J. Q., and Mishina, Y. (2008) *Development* **135,** 3801–3811

37. Janssens, K., ten Dijke, P., Janssens, S., and Van Hul, W. (2005) *Endocr. Rev.* **26,** 743–774

38. Murakami, T., Yamamoto, M., Ono, K., Nishikawa, M., Nagata, N., Motoyoshi, K., and Akatsu, T. (1998) *Biochem. Biophys. Res. Commun.* **252,** 747–752

39. Thirunavukkarasu, K., Miles, R. R., Halladay, D. L., Yang, X., Galvin, R. J., Chandrasekhar, S., Martin, T. J., and Onyia, J. E. (2001) *J. Biol. Chem.* **276,** 36241–36250

40. Karst, M., Gorny, G., Galvin, R. J., and Oursler, M. J. (2004) *J. Cell. Physiol.* **200,** 99–106

41. Erlebacher, A., and Derynck, R. (1996) *J. Cell Biol.* **132,** 195–210

42. Filvaroff, E., Erlebacher, A., Ye, J., Gitelman, S. E., Lotz, J., Heillman, M., and Derynck, R. (1999) *Development* **126,** 4267–4279

43. Subramaniam, M., Gorny, G., Johnsen, S. A., Monroe, D. G., Evans, G. L., Fraser, D. G., Rickard, D. J., Rasmussen, K., van Deursen, J. M., Turner, R. T., Oursler, M. J., and Spelsberg, T. C. (2005) *Mol. Cell. Biol.* **25,** 1191–1199

44. Okamoto, M., Murai, J., Yoshikawa, H., and Tsumaki, N. (2006) *J. Bone Miner. Res.* **21,** 1022–1033

45. Judge, D. P., Biery, N. J., Keene, D. R., Geubtner, J., Myers, L., Huso, D. L., Sakai, L. Y., and Dietz, H. C. (2004) *J. Clin. Invest.* **114,** 172–181

46. Mohammad, K. S., Chen, C. G., Balooch, G., Stebbins, E., McKenna, C. R., Davis, H., Niewolna, M., Peng, X. H., Nguyen, D. H., Ionova-Martin, S. S., Bracey, J. W., Hogue, W. R., Wong, D. H., Ritchie, R. O., Suva, L. J., Derynck, R., Guise, T. A., and Alliston, T. (2009) *PLoS One* **4,** e5275